

Caustics-induced coalescence of small droplets near a vortex

P. Deepu,^{1,*} S. Ravichandran,^{2,†} and Rama Govindarajan^{3,‡}

¹*Department of Mechanical Engineering, Indian Institute of Technology, Palakkad 678557, India*

²*TIFR Centre for Interdisciplinary Sciences, Narsingi, Hyderabad 500075, India*

³*International Centre for Theoretical Sciences, TIFR, Bangalore 560089, India*

(Received 30 June 2016; published 28 February 2017)

How droplets grow rapidly from 10 to 50 μm is an outstanding question in cloud physics. We show theoretically and numerically that caustics, locations of multivalued droplet velocity, of *small* droplets near a *single* planar steady vortex offer one route through this bottleneck. Such a vortex serves as a simple model for the more complicated turbulence field existing in clouds. Within a special radial distance r_c from the vortex center, droplets closer to the vortex can centrifugally overtake those farther out and coalesce. Small polydispersity increases r_c dramatically, enabling repeated collisions at short time intervals and formation of large droplets. Our results show that caustics brought about in a polydisperse suspension could offer a mechanistic explanation of accelerated rain initiation.

DOI: [10.1103/PhysRevFluids.2.024305](https://doi.org/10.1103/PhysRevFluids.2.024305)

I. INTRODUCTION

Particles suspended in turbulent flows exhibit inhomogeneous densities, even in statistically homogeneous turbulence [1]. Particles that are much denser than the fluid (“heavy” particles) are typically centrifuged out of regions of high vorticity and preferentially cluster in regions of high strain [2]. Such regions of high strain are normally associated with hyperbolic fixed points, but other kinds of attractors for heavy particles are known to exist. For example, if the vortex dynamics exhibits periodicity, particles can get attracted to elliptic fixed points in the rotating frame [3–5]. Further, the interaction of vorticity and gravity can change the dynamics [1,6] and produce stable limit cycles [7]. The problem of particle clustering, collisions, and coalescence in turbulent flows is relevant to many industrial and geophysical areas such as spray combustors, aerosol drug delivery, growth of water droplets in rain clouds, and formation of planetesimals in protoplanetary disks [8]. Our work addresses the droplet growth bottleneck in cloud physics, an open question on the rapidity of onset of rainfall in warm cumulus clouds. While diffusion-driven growth is relatively fast when the droplets are small ($<10 \mu\text{m}$), and collisions-coalescence driven by gravitational settling can explain growth beyond 50 μm , neither mechanism can explain the emergence of $\sim 50 \mu\text{m}$ drops from a 10 μm population within about 15 minutes [9]. We provide a mechanism for accelerated droplet growth in this size range.

The coupling between small heavy particles and the flow is characterized by the Stokes number, $St \equiv \tau/\tau_f$, where τ is the response time of the particle (defined later) and τ_f is a typical flow time scale, such as a vortex turnover time. Droplets of Stokes numbers above a critical value (≈ 1 based on the Kolmogorov timescale [10]) respond to flow structures in the dissipative range of turbulence, and experience caustics, i.e., two or more particles with different velocities arrive at the same place at the same time. Caustics are thought to play an important role in clustering (see, e.g., Ref. [11]) and therefore in increasing collision rates (see, e.g., Ref. [12]). Such collisions typically take place between particles being propelled out of different vortical regions at large relative velocities [13]. The term “caustics” in common parlance is thus evocative of relatively *large* particles and regions *between* vortices.

*deepu@iitpkd.ac.in

†ravis@tifrh.res.in

‡rama@icts.res.in

Our interest is in small and heavy droplets, in the vicinity of a *single* vortex. Here too caustics can occur, as shown by Ref. [14], for particles which start within a critical radius r'_c from the vortex center, which, for a pair of identical particles is $r'_c = 0.55\sqrt{2\pi\Gamma\tau}$, $2\pi\Gamma$ being the circulation of the vortex. [When not clear from the context, a prime will be used to indicate a dimensional variable.] We ask whether such caustics can affect the rate at which droplets grow, and answer strongly in the affirmative. We show that droplets which begin life at a radius within r'_c of the vortex centre are far more likely to collide and coalesce than droplets which lie outside. The present study uses a two-dimensional, time-independent vortex as a model for turbulent eddies. This is an oversimplification since vortices evolve in space and time in a turbulent flow; however, it leads to a nontrivial yet tractable model describing the basic features of turbulence-particle interaction. It also brings to light evidence that the neighborhood of each vortex can be important for caustics formation.

Our results also show that the caustics radius r_c for the smallest polydispersity in droplet size is different by orders of magnitude from that for identical droplets, so slightly larger particles, as they are centrifuged out, can mop up a large number of smaller particles in an extremely short time, to effect runaway growth. This further suggests that initially polydisperse systems of particles would undergo collisions and produce large droplets more frequently. We confirm this prediction by numerical simulations. Thus a vast majority of the large droplets seen in the flow are those in which caustics have initiated the growth.

Droplet dynamics within the caustics radius r_c may not be described by a field [15], since velocity can be multivalued at a given place and time. Outside this radius, droplet dynamics may be described by a compressible field, where the divergence $\nabla \cdot \mathbf{v}_p < 0$, so droplets come closer to each other slowly. Thus collisions outside the caustics radius may occur when the centres of two droplets approach closer than the sum of their radii, but these will be seen below to be rare events. We use the terms “particle” and “droplet” interchangeably, because our droplets are so small that they remain practically spherical and are made up of fluid which is much more viscous than the surroundings, so that standard Stokes flow around each droplet is an adequate description, which is discussed further below.

II. FORMULATION OF THE MODEL

Since our interest lies in the bottleneck range of droplet sizes, we disregard the effect of gravity (for studies on this effect, see Ref. [16]). The only force applied on the droplet is Stokesian drag. This is a simplifying assumption, since in our numerical simulations, particle Reynolds numbers up to $O(1)$ are observed, and in these cases an Oseen correction to the Stokes drag would become appropriate. The viscous relaxation time scale (or Stokes time) of a droplet of radius $a(t)$ is given by $\tau(t) = 2\rho_p a(t)^2 / \rho\nu$. Here ρ_p is the particle density, ρ is the density of the fluid, ν is its kinematic viscosity, and t is time. Under these assumptions, for heavy ($\rho_p \gg \rho$) and small [$a(t) \ll$ the relevant flow length scales] particles, Maxey-Riley equations reduce to $\dot{\mathbf{x}} = \mathbf{v}$ and $\dot{\mathbf{v}} = \frac{1}{\tau(t)}[\mathbf{u}(\mathbf{x}, t) - \mathbf{v}]$, where $\mathbf{x}(t)$ is the position vector of the particle.

The fluid flow field $\mathbf{u}(\mathbf{x}, t)$ is prescribed by a steady planar point vortex with circulation $2\pi\Gamma$. After recasting the above equations in cylindrical polar (r, θ) coordinates with origin at the vortex center, and using $\tau(0)$ and $\sqrt{\Gamma\tau(0)}$ to nondimensionalize time and length respectively, we get

$$\ddot{r} + b(t)\dot{r} = \zeta^2/r^3, \quad (1)$$

$$\dot{\zeta} + b(t)\zeta = b(t), \quad (2)$$

where $b(t) = [a_1/a(t)]^2$, with $a(t=0) = a_1$, is a staircase function that undergoes a step change with every coalescence event. Its introduction allows us to study the interplay between caustics and coalescence, which was not addressed in previous studies [14, 17]. Upon putting $b(t) = 1$, Eqs. (1) and (2) respectively reduce to Eqs. (8) and (9) in Ref. [14]. $\zeta = r^2\dot{\theta}$ denotes the angular momentum

per unit mass of the particle about the vortex center. The overdot represents differentiation with respect to time. Particles which start within r_c will be flung out and overtake all particles that were initially located within a critical radial separation. We show by a singular perturbation analysis that particles which start at $r \gg 1$ cannot overtake any others, particles which start at $r \ll 1$ can overtake those which start at $r \gg 1$, and that there is a critical radius of order 1 where the behavior changes. For an initial particle velocity equal to the local fluid velocity, Eq. (2) gives $\zeta(t) = 1$. For simplicity, we ignore collisions and set $b(t) = 1$. Subsequently, Eq. (1) becomes amenable to analytical solutions in two asymptotic limits. At large r and t , the inertia term (first term) can be neglected. With the initial radius $r(0) = r_o$, it leads to the outer solution

$$r^4 - r_o^4 = 4t. \quad (3)$$

In the other asymptotic limit of short time and radius, the Stokes drag (second) term can be ignored in favor of the other two terms. The resulting differential equation, along with the initial condition $r(0) = r_i$, admits the following inner solution at large $r - r_i$:

$$r_i(r - r_i) = t. \quad (4)$$

The crossover between the two asymptotic limits of small and large r can be shown to take place at $r_c \sim O(1)$.

Though Eqs. (3) and (4) are strictly applicable only at the two asymptotic bounds, they are useful for presenting a simple description of caustics, as follows. We observe that the inner solution describes a rapid ejection of the particle ($r \propto t$), while the outer solution corresponds to a slow radial velocity. Hence, a particle that started from r_i will catch up with the one that started from $r_o(\gg r_i)$.

III. METHODOLOGY

Thus caustics enable droplets to collide with each other at significant relative velocities, thereby aiding droplet growth through coalescence. To quantify the proportion of large droplets that are formed due to caustics, we numerically simulate Eqs. (1) and (2) for a multidroplet system. To avoid the singularity at the center of a point vortex, we use the more realistic Lamb-Oseen vortex to model the fluid tangential velocity as $u_\theta = (1 - e^{-r^2/r_v^2})/r$. The droplets are initially randomly positioned in a plane perpendicular to the vortex axis around the vortex center within a radius of R , which is taken to be a few multiples of r_c . The Lagrangian trajectories of the particles are tracked using a fourth order Runge-Kutta method. Simulations are conducted over an ensemble of random initial droplet configurations. For example, the polydisperse system results presented below are from 50 realizations with a total number of particles $N = 3 \times 10^5$.

We choose parameters typical of warm clouds. We set the average initial droplet radius to $10 \mu\text{m}$ with a prescribed polydispersity in size, and the droplet planar number density, n to $4000/\text{m}^2$, corresponding to a cloud liquid content of about $0.5 \text{ g}/\text{m}^3$ or roughly one droplet per Kolmogorov volume, and a collision cross section of one particle diameter. Evidently, increasing the number density and/or droplet diameter will increase the frequency of droplet collisions and accelerate the droplet growth rate, but such a parametric study is outside the scope of this paper. In the spectrum of a real cloud, circulation would range from $\sim 10^{-5} \text{ m}^2/\text{s}$ (at the Kolmogorov length scale, $r_k \sim 1 \text{ mm}$) to $100 \text{ m}^2/\text{s}$ (at the integral length scale of 100 m [9]). In our short simulation times, the probability of observing collision events is very low for $\Gamma \lesssim 1 \text{ m}^2/\text{s}$ (as the caustics zone shrinks significantly), whereas for $\Gamma \gtrsim 10 \text{ m}^2/\text{s}$ the particle velocities would be too large for Stokes drag to be applicable. Hence, for the purposes of illustration, we simulate for two values of circulation: $\Gamma = 1 \text{ m}^2/\text{s}$ and $\Gamma = 10 \text{ m}^2/\text{s}$, and set $r_v = 0.3$. We note that these values of circulation describe intense vorticities corresponding to high-intermittency events which typically take the form of long-lived vortex filaments [18,19]. The corresponding Stokes number = $O(10)$ based on the maximum vorticity. Note that the numerical value of the Stokes number is high because the vortex turnover time scale is low, but the droplets are too small to display significant settling under gravity.

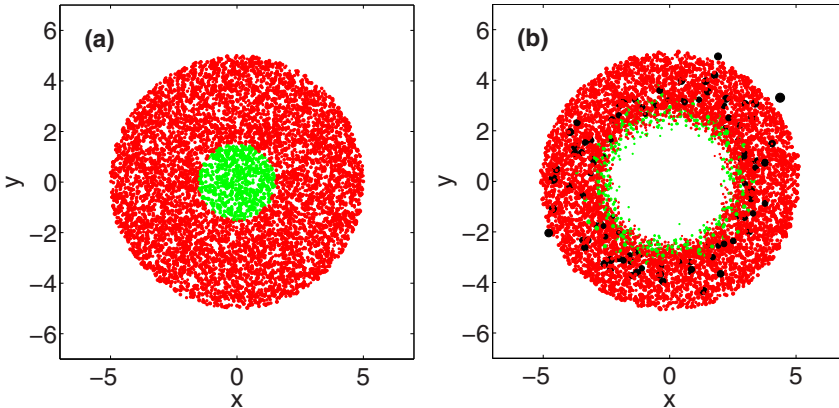


FIG. 1. (a) Snapshot of the initial locations of the droplets (randomly distributed) with a mean size of $10 \mu\text{m}$ and standard deviation of $2 \mu\text{m}$. (b) Droplet positions at $t' = 0.024$ s. $\Gamma = 10 \text{ m}^2/\text{s}$. Origin represents the center of the vortex. The droplets which start their journey from within the critical radius of caustics are colored green (dark grey), others red (light grey). Subsequently if in a merging event, at least a caustics droplet is involved, the resulting droplet is colored black. The size of the black droplets is scaled up for better visualization.

Given the low particle volume fraction, only binary collisions are assumed to take place. At the beginning of every simulation time interval $[t, t + \Delta t]$, all pairs of droplets (i, j) are checked for potential collision by calculating the time $\Delta t^{(ij)} = ((a^{(i)} + a^{(j)}) - r^{(ij)})/v^{(ij)}$, at which they would touch if they continued to move in straight trajectories. The superscript (ij) denotes a relative quantity between the i th and j th droplets. If $0 < \Delta t^{(ij)} < \Delta t$, the droplets are deemed to collide at $(t + \Delta t^{(ij)})$. For more details, see Ref. [20]. However, not all collisions need result in coalescence; for instance, if the droplets do not approach each other with sufficient kinetic energy to expel the intervening air film, they will bounce away. Based on approach conditions such as collision angle, relative velocity between the colliding droplets and the ratio of droplet sizes, we determine whether two colliding droplets will bounce or merge (see Ref. [21] for details). Since cloud droplets are small ($a < 100 \mu\text{m}$), the probability of fragmentation on collision is neglected [22]. Bounce and coalescence events are treated as elastic and inelastic collisions, respectively, with droplets always remaining spherical.

IV. RESULTS AND DISCUSSION

For brevity we refer to droplets located initially within $r_c = 0.55\sqrt{(2\pi)}$ as caustics droplets. We color these droplets green and other droplets red [Fig. 1(a)]. In the course of the simulation, droplets resulting from coalescence events involving at least one caustics droplet are colored black and remain black subsequently. The fraction of large droplets at the end of the simulation which are black give a measure of coalescence induced by caustics.

In Fig. 1 we present the snapshots of droplet positions at the beginning and end of a typical simulation (see also movie 1 in the Supplemental Material [23]). The simulation time is chosen long enough for most of the high-velocity particles to overtake the outer slow-moving particles [see Fig. 1(b)], beyond which almost no more collision events are expected to occur. The large droplets, which are centrifuged out the farthest (order of metres in a fraction of a second), are invariably black, i.e., caustics droplets were involved in their creation. Note that the time taken is far shorter than a typical lifetime of vortices of such circulations in turbulent flows of Reynolds numbers typical of a cloud. Though large droplets form only a small fraction of the total population, a dramatic change this causes in the caustics radius, as shown below, will lead to significant droplet growth.

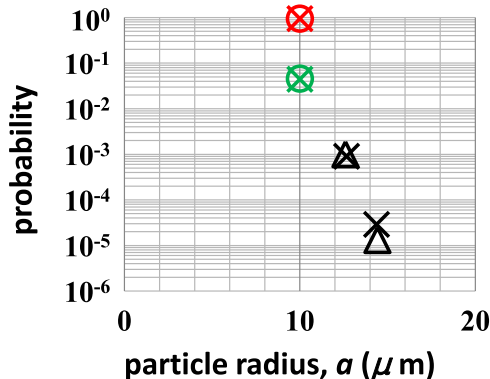


FIG. 2. Probability distribution of droplet size for an initial monodisperse population at $t = 0$ (\circ) and $t = 0.044$ s (\times). $\Gamma = 1\text{m}^2/\text{s}$. Theoretical predictions from Eq. (5), using the same values of R' and N_c/N as used in simulation are shown by Δ . The same color coding as in Fig. 1 is used.

A. Collisions in a monodisperse population

Initially monodisperse droplets too grow similarly, with caustics droplets being overwhelmingly more successful in triggering coalescence, but the population of larger droplets is smaller than in the polydisperse case. The evolution of an initially monodisperse population is described in Appendix A. Briefly, we first derive the probability of collision between a j -mer (droplet of size a_j) and a monomer [see Eq. (A1)] and subsequently the survival probability of a j -mer as it travels from r'_{j-1} (the radius location where the last collision has occurred) to a given r' . Finally, $P(a_q, r')$, the probability of a monomer which starts at r'_c growing to a q -mer at position r' is obtained by multiple integration of the appropriate product of survival and collision probabilities over successive intervals of radii between collisions [see Eq. (A2)]. Treating coalescence events as statistically independent, the probability of finding a q -mer in the population initially spread over a radius of R' is

$$\mathcal{P} \approx P(a_q, R') N_c / N, \quad (5)$$

where N_c/N is the initial fraction of caustics droplets and denotes the probability that a given monomer is a caustics droplet. This theoretical prediction is seen in Fig. 2 to be in excellent agreement with numerical simulations. There is thus a significant probability of coalescence giving rise to lower-order mergers in a short time. At larger time and radius, the probability of production of large droplets will be even higher. Note that our theory allows only the caustics droplets to grow in size, and hence the observed match reinforces the conclusion that caustics droplets are responsible for large droplet production. Thus we have shown that caustics near a single vortex can transform a monodisperse aerosol into a polydisperse population, with significant population of larger particles. We show next how the small degree of polydispersity thus generated can have a drastic effect on the caustics radius and thence on the number of droplets with which a given droplet can collide, initiating a domino effect.

B. Effect of polydispersity

In Eqs. (1) and (2), we allow for two droplets at an initial radial separation of δr to have different Stokes times (τ_i and τ_o , for inner and outer). The critical caustics radius r_c , i.e., the maximum radius at which an inner droplet placed initially may overtake at least the droplet in front for any δr , is shown as a function of the ratio $\xi \equiv \tau_o/\tau_i$ in the inset to Fig. 3. At $\xi = 1$, we recover the result of $r_c = 1.38$ for the mono-disperse case; but the main finding here is that r_c is very different when the lighter droplet is at the rear than when it is in the front. At $\xi = 0.99$, for example, the critical radius

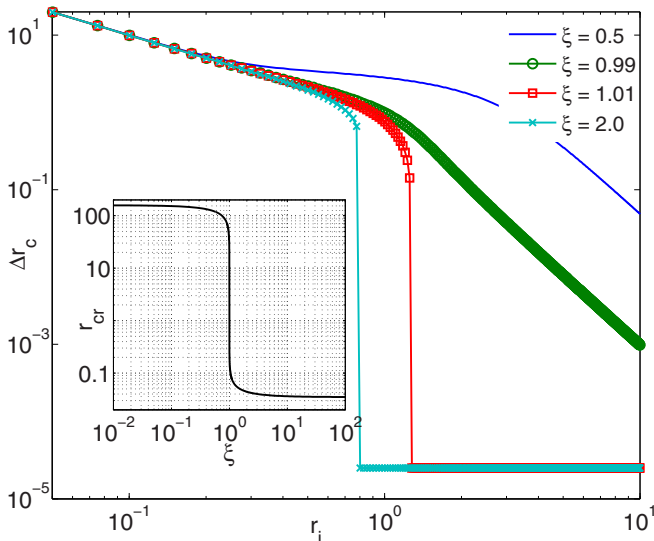


FIG. 3. Effect of bidispersity in particle size on the maximum distance that can be bridged (within the chosen time span of integration) as a function of initial radius at different values of ξ , as given in the legend. Inset: Effect of bidispersity on the critical radius for caustics at $\delta r = \sqrt{(2\pi)} \times 10^{-5}$. τ_i is used for nondimensionalization.

is 2 orders of magnitude larger than the critical radius for $\xi = 1$. The droplet at the rear will overtake, and thus has the possibility of coalescing with, all droplets within a critical initial separation Δr_c (for more details, see Ref. [14]). This is shown in Fig. 3. The difference between the curves for $\xi = 0.99$ and $\xi = 1.01$ reiterates that caustics harness even the slightest polydispersity to enable a much larger number of droplets to participate in the collisions-coalescence process. Further, mechanisms such as supersaturation fluctuations in clouds can encourage a degree of polydispersity [24] and contribute to a much larger caustics region. This in turn increases the collision rate and permits generation of larger droplets. Extending the theoretical analysis carried out for the monodisperse case [Eq. (A2)] to a more realistic polydisperse case will be highly complicated. Nevertheless, in the case of a bidisperse system, one can derive a closed form expression for the probability of survival of an inner (and bigger) droplet as it overtakes the outer (smaller) particles. We defer this discussion until after we have presented the numerical results.

Shown in Fig. 4 for two typical circulations is the droplet size distribution (averaged over many realizations) after a small simulation time. An initially polydisperse system with a Gaussian size distribution of mean $10 \mu\text{m}$ and standard deviation $2 \mu\text{m}$ has been prescribed, as shown for comparison. It is clear that, first, caustics-induced mergers produce size distributions (black curves) with larger mean values and extended tails. In stark contrast, the probability distributions for droplet starting outside the caustics zone hardly change. Second, the coalescence rate increases significantly at higher Γ due to a bigger caustics zone and greater particle ejection rate. Finally, droplets that are initially larger are more vulnerable to collisions and merging. It is evident that polydispersity increases the chance of obtaining larger droplets. We observe an increase in standard deviation of droplet size by more than 4% for $\Gamma = 10 \text{ m}^2/\text{s}$ in less than 0.2 s (0.2% for $\Gamma = 1 \text{ m}^2/\text{s}$ in 0.4 s) in the case of a polydisperse system.

C. Evolution of droplet size at large times

Using high values of vorticity corresponding to highly intermittent events allowed us to demonstrate the effects of caustics in simulation times as short as $\approx 0.01 \text{ s}$, as opposed to the bottleneck timescale of 15 minutes. For large times, we may use Eq. (5) to make an analytical

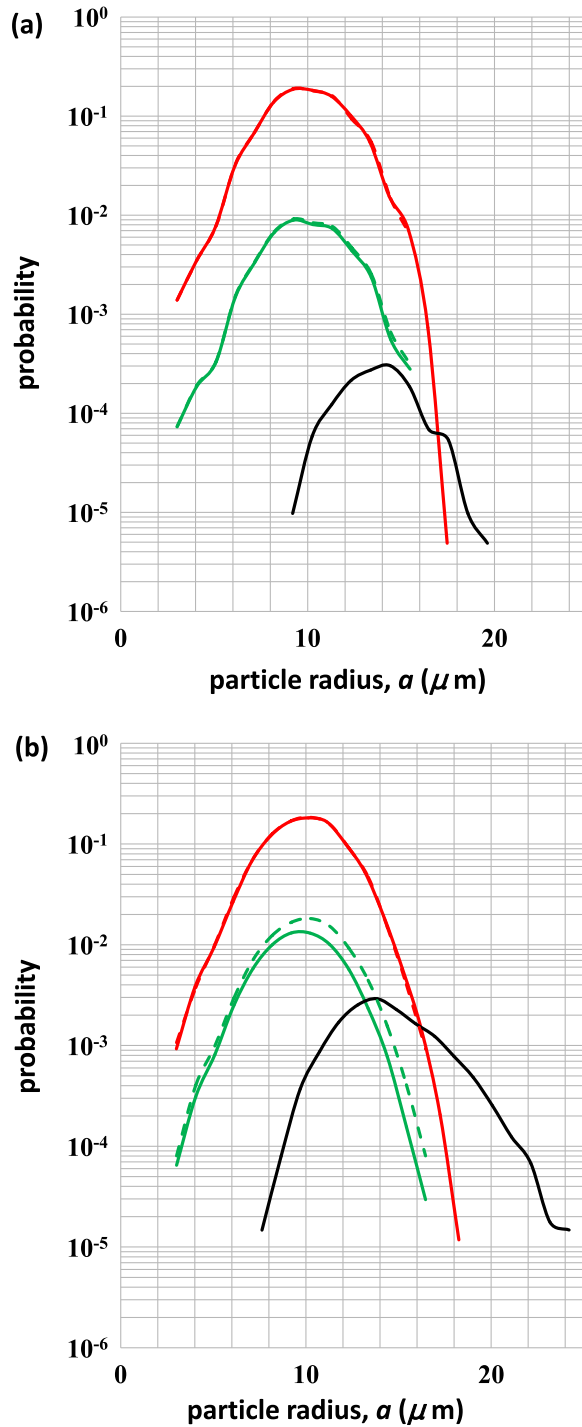


FIG. 4. Initial (solid line) and final (dashed line) probability distribution of droplet size for an initial polydisperse population. (a) $\Gamma = 1 \text{ m}^2/\text{s}$, simulation time = 0.044 s. (b) $\Gamma = 10 \text{ m}^2/\text{s}$, simulation time = 0.024 s. The same color coding as in Fig. 1 is used.

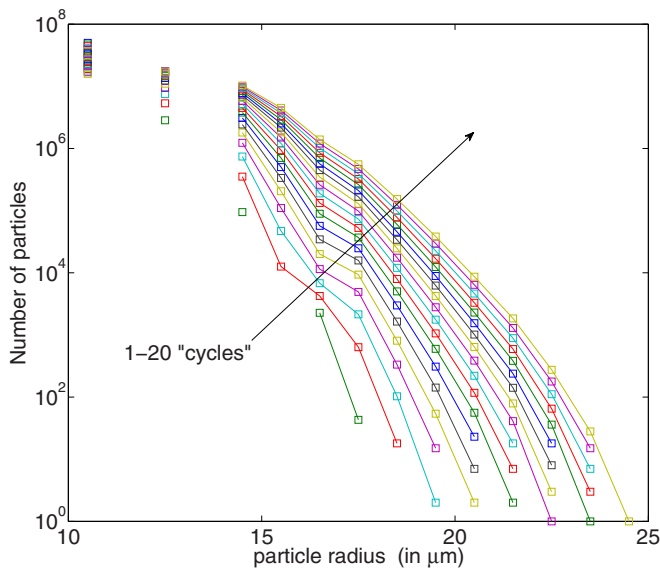


FIG. 5. An estimate of the evolution of droplet size distribution at later times. A monodisperse initial population of droplet radius $10 \mu\text{m}$ and a representative $\Gamma = 1.6 \text{ m}^2/\text{s}$ are used.

estimation of droplet growth. In turbulent flows, a given droplet can participate in a succession of caustics of different vortices. We allow 5×10^8 droplets to grow through caustics up to a distance of 10 times the caustics radius. At this distance, we deem the droplets to be in the thrall of another vortex, randomize their locations, and allow growth again in a new cycle. Just for demonstration, we take $N_c/N = 0.1$ in Eq. (5), amounting to assuming that about 10% of the flow has coherent structures. We show in Fig. 5 the evolution of the droplet size distribution under such a sequence. Taking the time for each cycle to be determined by droplets in the bin of largest inertia, the 20 cycles shown in Fig. 5 would take about 1000 s, or about 15 minutes, at which time there are ≈ 2000 droplets of $22 \mu\text{m}$, and $\approx 40\,000$ droplets of $20 \mu\text{m}$.

D. Collisions due to inertial-range vortices

From the results shown in Fig. 4, we obtain maximum droplet radius growth rates of the order of tens of $\mu\text{m}/\text{s}$ for Γ of order $1 \text{ m}^2/\text{s}$ or more (contrast this with the average droplet growth rate of $\approx 0.01 \mu\text{m}/\text{s}$ needed to explain the cloud bottle-neck problem; e.g., see Ref. [25]). But such a high growth rate is obtained from simulations carried out with intense vorticities; hence in reality we expect much lower droplet growth rates. We now discuss typical vortices consistent with the classical Kolmogorov picture, where the circulation of a vortex is fixed by its length scale ($\Gamma \propto r_v^{4/3}$). Here collisions in a monodisperse population would be very rare during the vortex lifetime T (which we take to be 10 times the rotation time of the vortex). In the more realistic case of polydisperse populations, the caustics zone has been seen to be orders of magnitude larger, and in Appendix B, the number of collisions in a bidisperse population is estimated analytically. In Fig. 6 we present the number of bigger droplets per unit volume that undergo at least one collision, $N_{C>0}$, as a function of Γ and T for a bidisperse system. It is seen that the number of droplets which undergo collisions scales as $\Gamma^{5/8}$. In Appendix B, we show in detail that the reason for this scaling is that for a dilute system, $N_{C>0}$ will scale as the radius where the inner (and bigger) particle reaches in time T , $r_i(T)$, which itself can be shown to scale as $\Gamma^{5/8}$. From the foregoing discussion, it is clear that the concerted action of caustics and polydispersity in the vicinity of moderate vortices results in non-negligible number of droplet collisions and thus could provide a mechanism to bridge the bottleneck.

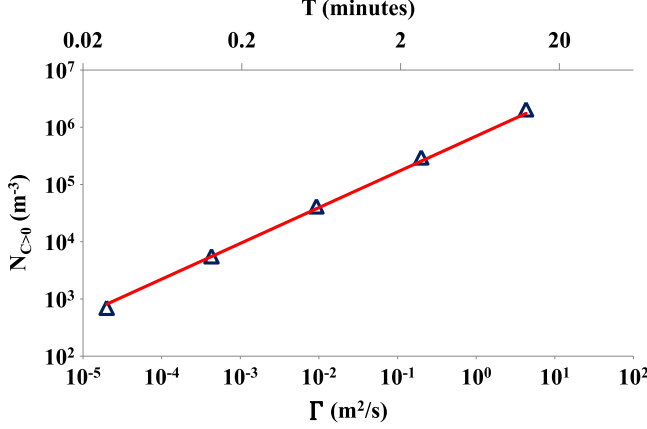


FIG. 6. Number of bigger droplets (per unit volume) in an initial bidisperse system ($\xi = 0.81$) which undergo at least one collision as a function of circulation and lifetime of the vortex. Markers: Eq. (B6); solid line: power law, $N_{C>0} \propto \Gamma^{5/8}$. Half of the 10^8 droplets present in 1 m^3 volume of a typical cloud is assumed to be bigger particles and the rest smaller.

V. CONCLUSIONS

We have shown that caustics near a planar time-independent vortex can contribute significantly to rapid growth of small droplets. An overwhelming majority of small-droplet collisions involve at least one caustics droplet. Since the caustics region is very large with even small polydispersity, droplets which have undergone at least one coalescence have a far superior chance of repeated collisions and runaway growth in a very short time, even in a dilute suspension. The strength of our theory is its simplicity, and it explores a droplet dynamics regime where few direct measurements have been made. We hope that our findings will motivate such efforts, in particular to estimate the role of caustics, not only in clouds, but in other applications as well. Finally we remark that it would be presumptuous to claim that we have solved the bottleneck problem using our simplified picture of turbulent flows; however, it is fair to say that we have been successful in demonstrating the potential of caustics-induced coalescence for producing large droplets in short times by strong vortices. The growth of droplets in a realistic cloud setting, accounting for the effect of caustics, is yet to be explored.

ACKNOWLEDGMENT

We are thankful to the TIFR Centre for Interdisciplinary Sciences, Hyderabad, where this work was begun, for support.

APPENDIX A: PROBABILITY OF PRODUCTION OF A q -MER IN A MONODISPERSE POPULATION

The most likely collisions are those between droplet A of radius a_j and droplet B of radius a_1 . The subscript j indicates a droplet made up of j initial droplets. As droplet A moves from r' to $r' + \Delta r'$, the probability, p , of colliding (and coalescing) is given by

$$p_j = n2\pi r' \Delta r' \frac{a_j + a_1}{2\pi r'} = n \Delta r' a_1 (j^{1/3} + 1) \equiv f_j \Delta r'. \quad (\text{A1})$$

Mass conservation on every coalescence event stipulates $a_j/a_1 = j^{1/3}$. The probability of survival of droplet A, i.e., of retaining its size as a_j , is $(1 - p_j)$. With r'_{j-1} being the radial distance where the $(j - 1)$ -th collision has occurred, the probability of survival up to r' , in the limit of small $\Delta r'$,

becomes $S(r', r'_{j-1}) = \exp[-na_1(r' - r'_{j-1})(1 + j^{1/3})]$. Since all droplets within the caustics region reach r'_c at a very short time, we prescribe this as the starting location. For multiple successive collisions, the probability of a flung-out monomer (of size a_1) growing to a q -mer (of size of a_q) at a distance r' , due to the $(q - 1)$ collisions it has undergone while traveling out from r'_c to r' , is given by

$$P(a_q, r') = \int_{r'_{q-1}=r'_c}^{r'} \int_{r'_{q-2}=r'_c}^{r'_{q-1}} \dots \int_{r'_2=r'_c}^{r'_3} \int_{r'_1=r'_c}^{r'_2} \prod_{j=1}^{q-1} [S(r'_j, r'_{j-1}) f_j] S(r', r'_{q-1}) \prod_{k=1}^{q-1} dr'_k. \quad (\text{A2})$$

APPENDIX B: COLLISIONS IN A BIDISPERSE SYSTEM DUE TO INERTIAL-RANGE VORTICES

Consider an inner particle of radius a_{in} that starts from a radius r_0 and an outer particle of radius a_{out} starting from r . As seen in Fig. 3, if $a_{\text{in}} > a_{\text{out}}$, the caustics radius could be of the order of 100. We restrict this discussion to $r > 1$, which allows us to use the far-field expressions [Eq. (3)] for the droplet velocity. In this case, since both the droplets will have comparable velocities, we cannot assume the target (outer) particles to be stationary, unlike in the monodisperse case. If $\sqrt{\Gamma \tau_i}$ is taken to be the length scale for nondimensionalization, the radial position of the inner particle, r_{in} at time t is obtained from Eq (3), while that of the outer particle is given by

$$r_{\text{out}}^4(t) = r^4 + 4\xi t. \quad (\text{B1})$$

A collision is possible when the two particles reach a radius r_{coll} simultaneously. From the two equations, we may get this radial location as

$$r_{\text{coll}} = r_0 \left[\frac{\eta^4 - \xi}{1 - \xi} \right]^{\frac{1}{4}}, \quad (\text{B2})$$

where $\eta = r/r_0$. Then the probability of collision of the inner particle with an outer particle which started from within a ring of width Δr at r is given by

$$P_C(r, r + \Delta r) = n_{\text{out}} 2\pi r \Delta r \frac{a_{\text{in}} + a_{\text{out}}}{2\pi r_{\text{coll}}} = \frac{n_{\text{out}} \eta \Delta r a_{\text{in}} (1 + \sqrt{\xi})(1 - \xi)^{\frac{1}{4}}}{(\eta^4 - \xi)^{\frac{1}{4}}}, \quad (\text{B3})$$

where n_{out} is the number density of the outer particles.

In a given time T , the inner particle will reach $r_i(T)$ and will overtake all the outer particles which started initially from within a cutoff radius given by

$$r_{\text{max}} = \left\{ \xi + (1 - \xi) \left[\frac{r_i(T)}{r_0} \right]^4 \right\}^{\frac{1}{4}}. \quad (\text{B4})$$

Dividing the disk from r_0 to r_{max} into m rings, each of width Δr , the probability of survival (no collisions) of the inner droplet as it moves from r_0 to $r_i(T)$ is obtained as the product:

$$P_S(r_0, r_i(T)) = \prod_{k=1}^m [1 - P_C(r_0 + (k - 1)\Delta r, r_0 + k\Delta r)]. \quad (\text{B5})$$

Subsequently, the number density of the bigger droplets that undergoes at least one collision in time T is

$$N_{C>0} = [1 - P_S(r_0, r_i(T))] n_{\text{in}}, \quad (\text{B6})$$

where n_{in} is the number density of the bigger droplets.

Consider a time T proportional to the vortex turnover time $\tau_f = 2\pi/\omega$, where $\omega = 2\Gamma/r_v^2$ is the vorticity. From Kolmogorov scaling, we have $r_v^2 \sim \Gamma^{3/2} r_k^2 / v^{3/2}$; hence $T \propto \Gamma^{1/2}$. Note that $T/\tau_i \sim 1/\text{St}$. In dimensional terms, $r_i(T) = (r_0^4 + 4\tau_i\Gamma^2 T)^{1/4}$ and hence, for large enough $r_i(T)$, we have $r_i(T) \propto \Gamma^{5/8}$. Since $\xi < 1$, Eq. (B4) implies that $r_{\max} \sim r_i(T)$. Given the low volume fraction of cloud droplets, the probability of collision P_C in Eq. (B3) is very small and essentially invariant across the m rings. Therefore the product reduces to $A \exp[-Br_{\max}]$, where A and B are constants for a given r_0 . Using a linear approximation for this exponential leads to $N_{C>0} \propto \Gamma^{5/8}$.

-
- [1] K. Gustavsson and B. Mehlig, Statistical models for spatial patterns of heavy particles in turbulence, *Adv. Phys.* **65**, 1 (2016).
- [2] M. R. Maxey, The gravitational settling of aerosol particles in homogeneous turbulence and random flow fields, *J. Fluid Mech.* **174**, 441 (1987).
- [3] R. D. Vilela and A. E. Motter, Can Aerosols be Trapped in Open Flows? *Phys. Rev. Lett.* **99**, 264101 (2007).
- [4] J.-R. Angilella, Dust trapping in vortex pairs, *Physica D* **239**, 1789 (2010).
- [5] S. Ravichandran, P. Perlekar, and R. Govindarajan, Attracting fixed points for heavy particles in the vicinity of a vortex pair, *Phys. Fluids* **26**, 013303 (2014).
- [6] K. Gustavsson, S. Vajedi, and B. Mehlig, Clustering of Particles Falling in a Turbulent Flow, *Phys. Rev. Lett.* **112**, 214501 (2014).
- [7] A. M. Gañán-Calvo and J. C. Lasheras, The dynamics and mixing of small spherical particles in a plane, free shear layer, *Phys. Fluids A* **3**, 1207 (1991).
- [8] A. Johansen, J. S. Oishi, M.-M. Mac Low, H. Klahr, T. Henning, and A. Youdin, Rapid planetesimal formation in turbulent circumstellar disks, *Nature (London)* **448**, 1022 (2007).
- [9] W. W. Grabowski and L.-P. Wang, Growth of cloud droplets in a turbulent environment, *Annu. Rev. Fluid Mech.* **45**, 293 (2013).
- [10] M. Voßkuhle, A. Pumir, E. Lévêque, and M. Wilkinson, Prevalence of the sling effect for enhancing collision rates in turbulent suspensions, *J. Fluid Mech.* **749**, 841 (2014).
- [11] M. Wilkinson and B. Mehlig, Caustics in turbulent aerosols, *Europhys. Lett.* **71**, 186 (2005).
- [12] G. Falkovich, A. Fouxon, and M. G. Stepanov, Acceleration of rain initiation by cloud turbulence, *Nature (London)* **419**, 151 (2002).
- [13] K. Gustavsson and B. Mehlig, Distribution of relative velocities in turbulent aerosols, *Phys. Rev. E* **84**, 045304 (2011).
- [14] S. Ravichandran and R. Govindarajan, Caustics and clustering in the vicinity of a vortex, *Phys. Fluids* **27**, 033305 (2015).
- [15] M. Wilkinson, B. Mehlig, and V. Bezuglyy, Caustic Activation of Rain Showers, *Phys. Rev. Lett.* **97**, 048501 (2006).
- [16] B. J. Devenish, P. Bartello, J.-L. Brenguier, L. R. Collins, W. W. Grabowski, R. H. A. IJzermans, S. P. Malinowski, M. W. Reeks, J. C. Vassilicos, L.-P. Wang *et al.*, Droplet growth in warm turbulent clouds, *Q. J. R. Meteorol. Soc.* **138**, 1401 (2012).
- [17] R. A. Shaw, W. C. Reade, L. R. Collins, and J. Verlinde, Preferential concentration of cloud droplets by turbulence: Effects on the early evolution of cumulus cloud droplet spectra, *J. Atmos. Sci.* **55**, 1965 (1998).
- [18] R. Benzi and L. Biferale, Homogeneous and isotropic turbulence: A short survey on recent developments, *J. Stat. Phys.* **161**, 1351 (2015).
- [19] S. Douady, Y. Couder, and M. E. Brachet, Direct Observation of the Intermittency of Intense Vorticity Filaments in Turbulence, *Phys. Rev. Lett.* **67**, 983 (1991).
- [20] A. Dominguez, M. van Aartsijk, L. Del Castello, and H. J. H. Clercx, Aggregate formation in 3d turbulent-like flows, in *Particle-Laden Flow, From Geophysical to Kolmogorov Scales*, edited by B. J. Geurts, H. Clercx, and W. Uijttewaal, ERCOFTAC Series Vol. 11 (Springer, New York, 2007), pp. 359–371.

- [21] L. E. Kollár, M. Farzaneh, and A. R. Kerev, Modeling droplet collision and coalescence in an icing wind tunnel and the influence of these processes on droplet size distribution, *Int. J. Multiphase Flow* **31**, 69 (2005).
- [22] P. R. Brazier-Smith, S. G. Jennings, and J. Latham, The interaction of falling water drops: Coalescence, *Proc. R. Soc. London A* **326**, 393 (1972).
- [23] See Supplemental Material at <http://link.aps.org/supplemental/10.1103/PhysRevFluids.2.024305> for a movie showing particles near a vortex undergoing caustics-induced coalescence.
- [24] R. A. Shaw, Particle-turbulence interactions in atmospheric clouds, *Annu. Rev. Fluid Mech.* **35**, 183 (2003).
- [25] A. Pumir and M. Wilkinson, Collisional aggregation due to turbulence, *Annu. Rev. Condens. Matter Phys.* **7**, 141 (2016).